A C^1 FINITE ELEMENT FAMILY FOR KIRCHHOFF PLATE BENDING

J. TORRES, A. SAMARTÍN, V. ARROYO AND J. DÍAZ DEL VALLE

Departamento de Análisis de las Estructuras, Escuela Técnica Superior de Ingenieros de Caminos Universidad de Cantabria, Santander, Spain

SUMMARY

After a short introduction the possibilities and limitations of polynomial simple elements with C^1 continuity are discussed with reference to plate bending analysis. A family of this kind of elements is presented. These elements are applied to simple cases in order to assess their computational efficiency. Finally some conclusions are shown, and future research is also proposed.

INTRODUCTION

The application of the finite element method (F-E-M) to the analysis of Kirchhoff plate bending demands the continuity in the first derivative of the expansion of the deflection w. The reader is referred to Zienckiewicz's excellent book[1] for details.

The types of elements which satisfy this condition are referred to in the literature as conforming or compatible elements. However, it has been shown in References 2 and 3, that it is occasionally possible to obtain highly efficient converging results (with respect to the energy form) with non-conformingelements. This convergence, which in such cases may not be monotonic, may depend on the mesh configuration of finite elements, i.e. in some examples there may not be convergence. Irons[4] thus proposed his well-known patch test, that works for all 'non-pathological' situations.[5]

For bending compatible finite elements two important aspects of convergence—monotony and mesh independence—can be ensured without further tests, which in some cases are of practical and theoretical interest. However, the task of constructing conforming bending elements is not an easy one. In fact it is not possible to achieve C^1 conformity in simple elements by using polynomial expressions with unique expressions in their interior.[6] The several techniques developed up to this date for obtaining compatible elements 7–10 can be divided into two types, those considering C^1 compatibility and those avoiding it.

With C^0 there is no problem with the value of the second mixed derivative (w_{xy}) at the corners.

The second mixed derivative (w_{xy}) at the corners of the elements can be a function of other degrees of freedom (slave d.o.f.), or itself another degree of freedom (master d.o.f.). If the first case is considered, and only first derivatives are taken as master d.o.f.s at the corners, there are two possibilities to consider: (1) rational correcting functions and (2) division of the elements into areas (Figure 1).

Among the four types of solution shown in Figure 1, this paper deals with piecewise functions which, in addition to the general advantages of the FEM, provide a unified solution, easy changes of mesh (h-convergence), easy to impose boundary conditions and a symmetric

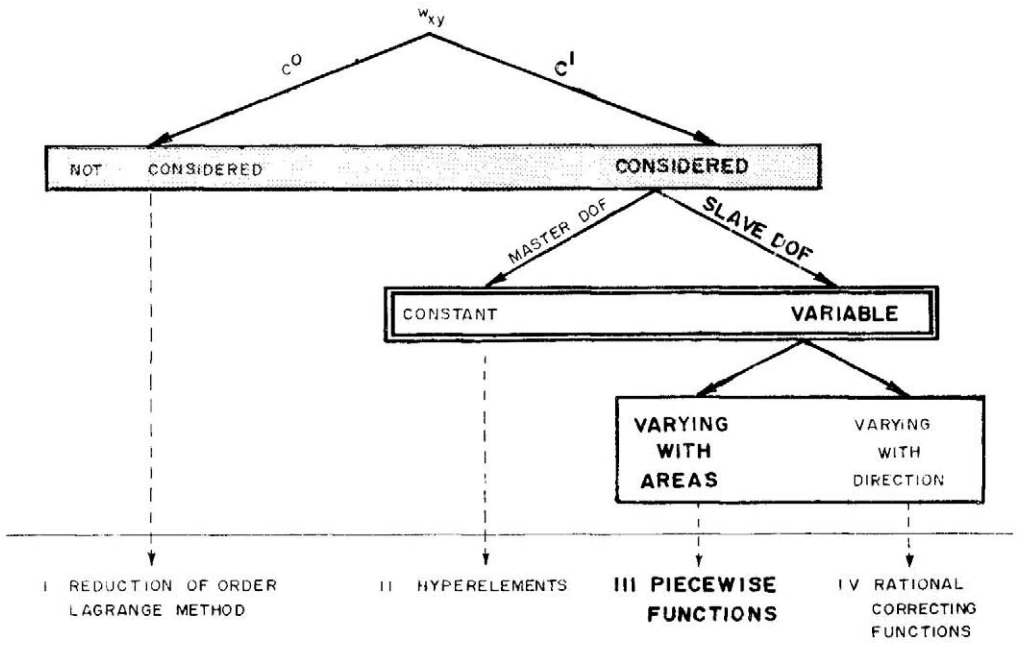

Figure 1. Techniques for obtaining compatible elements

banded matrix—and with C^1 elements about which, in addition to the advantages monotonous convergence and mesh independence it must be said that

1. The numerical integration can be very accurate because it is used in polynomials.
2. The extension to shells has no problems, so that the elements used are simple.[11]

A general procedure is proposed to construct the shape functions, so that an element family is achieved. In this way by varying the interpolation functions with the same mesh the accuracy is improved (h^k-convergence).

In the following a hierarchic family of C^1 elements based on the application of piecewise polynomials will be described. These piecewise polynomials were first used by Clough and Tocher[12] in triangular elements, and extended later to parallelograms by Clough and Felippa.[13] Triangular elements have also been used by Clough and Felippa.[13]

HIERARCHIC FAMILY

Introductory example

In order to grasp the main features of the family of triangular finite elements, the member corresponding to the polynomial order $N = 5$ will be considered.

The triangular element is divided into another three as is shown in Figure 2, where for simplicity '13' is the centre of gravity. In each of these subelements a complete polynomial interpolation function of degree 5 is built (Figure 2).

The number of degrees of freedom (d.o.f.) and their distribution along external and internal sides will be discussed. In each subelement 21 d.o.f. exist, corresponding to the number of polynomial coefficients. Along its external side the C^0 continuity is ensured by 6 d.o.f. and the C^1 continuity (first derivative in the normal direction to the side) demands 5 d.o.f. At each external corner there are only 3 d.o.f., namely w, $\partial w/\partial x$, $\partial w/\partial y$, because the element is simple.

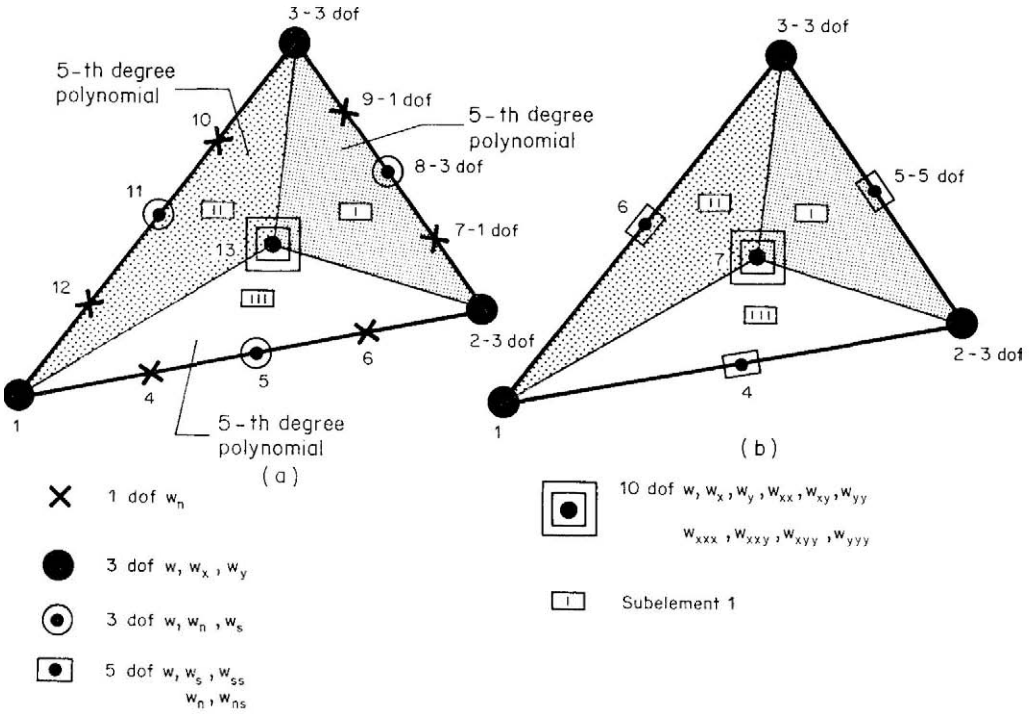

Figure 2. Two possible distributions of d.o.f. along the external sides of the 5th degree element

This means that 2 d.o.f. (w, $\partial w/\partial s$) and 1 d.o.f. ($\partial w/\partial n$) can be taken into account in the C^0 and C^1 continuity, respectively, along the external side. Then along this side, 2 ($= 6 - 2 \times 2$) d.o.f. and 3 ($= 5 - 2 \times 1$) d.o.f. for C^0 and C^1 continuity have to be considered (Figures 3(b), (c)), i.e. a total of 5 d.o.f. and therefore only 10 ($= 21 - 5 \times 3$) internal d.o.f. remain (Figure 2).

It is interesting to point out that several possibilities exist for placing the 5 ($= 2 + 3$) d.o.f. along the external side. All of them represent the same complete polynomial along the side and give identical approximation levels.[14] One corresponds to using only first derivatives along the side and is shown in Figure 2(a). Another possibility, perhaps the most simple one, is to concentrate all the 5 ($= 2 + 3$) d.o.f. at the midside node (Figure 2(b)).

A similar reasoning to the previous one allows us to concentrate the 10 remaining internal d.o.f. namely w, $\partial w/\partial x$, $\partial w/\partial y$, $\partial^2 w/\partial x^2, \ldots, \partial^3 w/\partial y^3$ (Figure 2) at the node 0. Then the continuity along each internal side will be analysed. First, C^0 continuity demands 6 d.o.f., but already at its two end nodes 6 d.o.f. = 2 d.o.f. ($w, \partial w/\partial s$) + 4 d.o.f. ($w, \partial w/\partial s, \partial^2 w/\partial s^2, \partial^3 w/\partial s^3$) exist (Figure 3(d)). This internal C^0 continuity always exists (Figure 4(a)). For the C^1 continuity 5 d.o.f. are needed. At the two end nodes there are 4 d.o.f. = 1 d.o.f. ($\partial w/\partial n$) + 3 d.o.f. ($\partial w/\partial n, \partial^2 w/\partial n\, \partial s, \partial^2 w/\partial n\, \partial^2 s$), (Figure 3). Therefore, in general, C^1 internal continuity does not exist. However it is possible to choose the internal d.o.f. at node '0' in such a way that this C^1 continuity exists. This means that 3 conditions (one for each internal side) should be imposed, or equally 3 d.o.f. should be expressed in terms of the remaining 7, and those of the external nodes, and then eliminated at the shape function level (Figure 4(b)). This step was first made analytically, but the expression became so complicated that it was decided to use a numerical procedure.

The element stiffness matrix is obtained by the addition of the subelement stiffness matrices. Afterwards it is possible to eliminate all the remaining 7 internal d.o.f. by static condensation of the element stiffness matrix (Figure 4(c)).

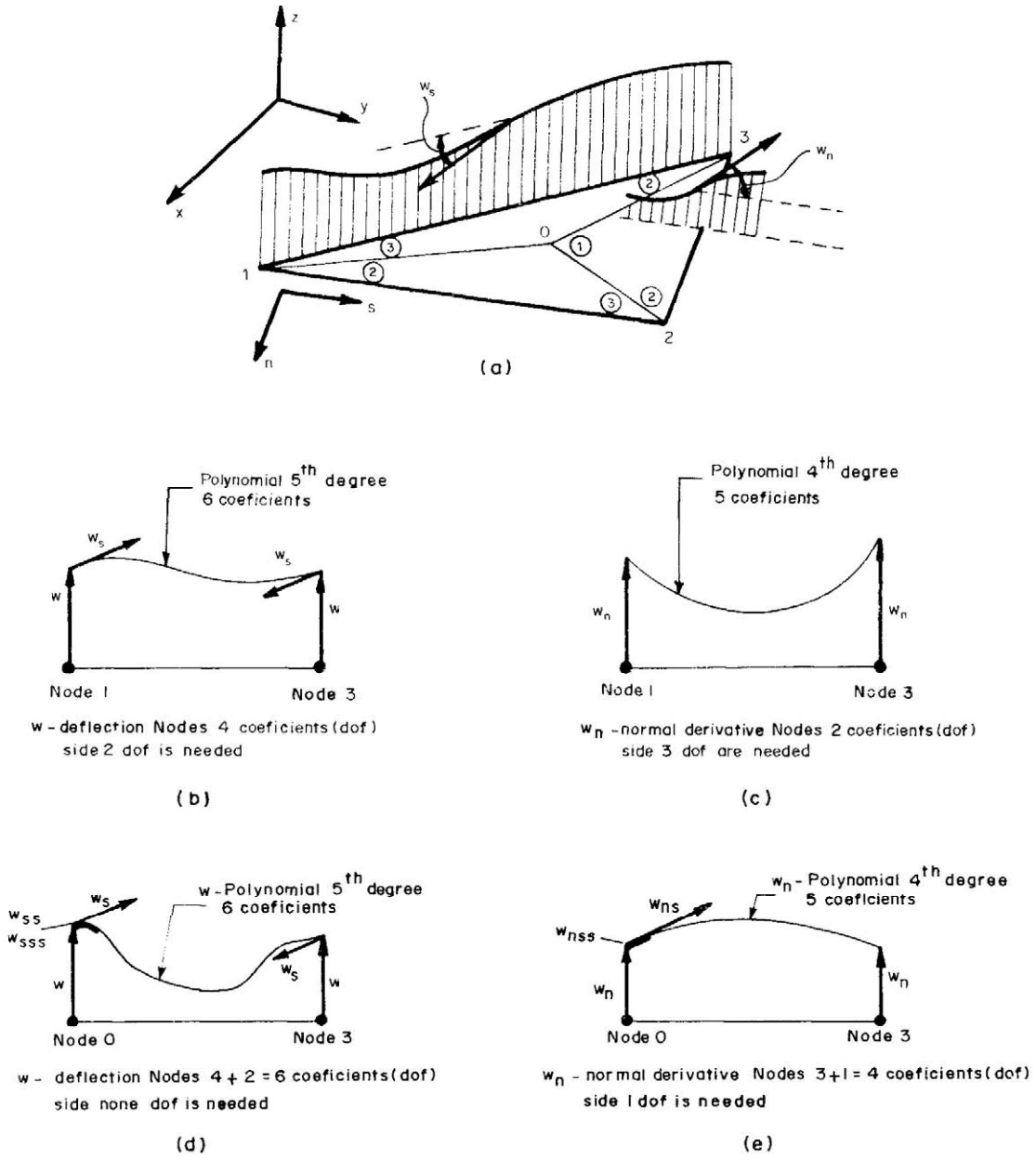

Figure 3. Continuity along external and internal sides: (b) w — deflection at the nodes — 4 coefficients (d.o.f.); 2 side d.o.f. are needed; (c) w_n — normal derivative at the nodes — 2 coefficients (d.o.f.) 3 side d.o.f. are needed; (d) w — deflection at the nodes — $4 + 2 = 6$ coefficients (d.o.f.); no side d.o.f. are needed; (e) w_n — normal derivative at the nodes — $3 + 1 = 4$ coefficients (d.o.f.); 1 side d.o.f. is needed

It is important to point out the fact that it is not possible to eliminate more than 3 internal d.o.f. at the shape function level by imposing C^2 or higher order of continuity along the internal sides.[15] This is because the element is simple and internal C^2 continuity produces the problem of the dependence among the d.o.f. owing to the unique value of $\partial^2 w/\partial s\,\partial n = \partial^2 w/\partial n\,\partial s$ at each vertex of the triangle.

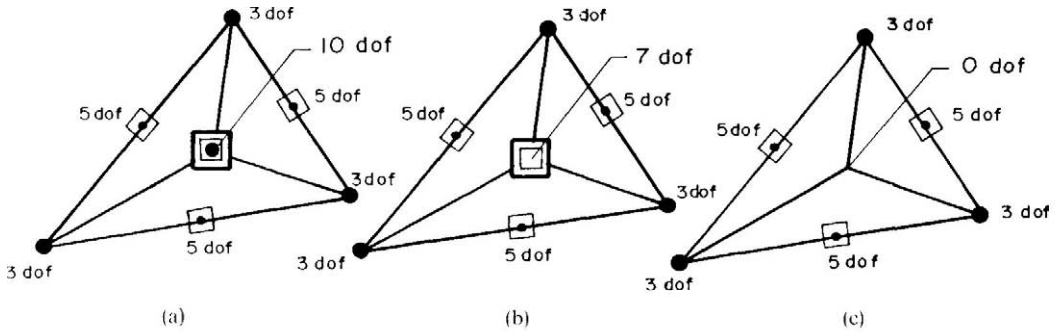

(a) (b) (c)

Figure 4. Derivations of the 5th degree element of the family: (a) element with internal continuity C^0 only — 34 d.o.f.; (b) internal d.o.f. eliminated at shape function level; internal C^1 continuity — 31 d.o.f., (c) internal d.o.f. eliminated by static condensation; internal C^1 continuity — 24 d.o.f.

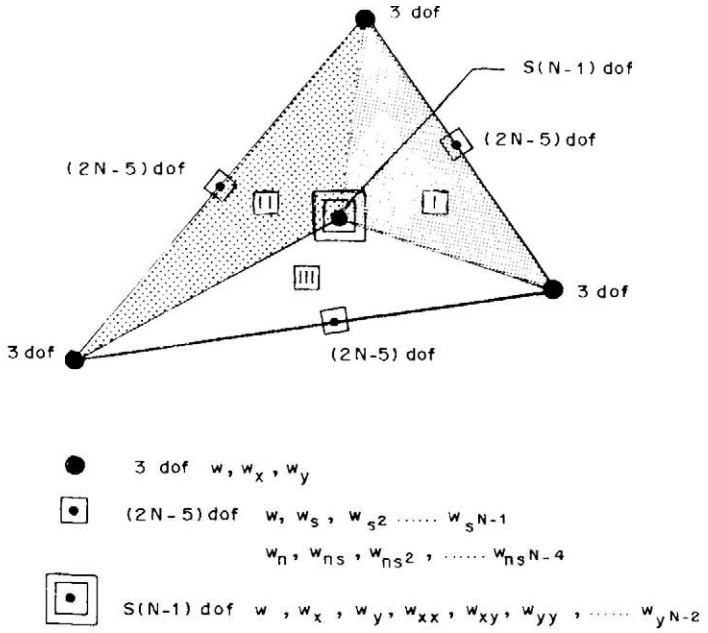

Figure 5. A general element N of the family with internal C^0 continuity only

Number and distribution of d.o.f. subelement interpolation function

The above ideas can be extended to a general member of the family of elements. The triangular element is divided into another three, as is depicted in Figure 5. In each of those subelements is built a complete polynomial interpolation function of degree N.

The number of d.o.f. and their distribution along external and internal sides will be discussed. The total number of d.o.f. in an Nth degree polynomial of two variables is

$$S(N+1)=\frac{(N+1)(N+2)}{2} \tag{1}$$

where $S(N)$ is the sum of the first N natural numbers.

First, along an external side the C^1 compatibility—in w and w_n—implies the results of Table I. For a polynomial of fifth degree this is explained in Figures 3(b) and 3(c).

The d.o.f. used at the central node of the external side are shown in Figure 6.

As the number of d.o.f. in the middle of an external side is $2N$-5 (Table I) the internal d.o.f. number will be

$$S(N+1) - 2 \times 3 - (2N-5) = S(N-1)$$

The continuity along an internal side is shown in Table II. One prescription of compatibility is imposed in order to obtain continuity in the normal derivative (w_n) Figure 3(e).

The condition used here is to match the normal derivative between subelements in the middle of the internal sides, that is

$$\begin{aligned} w_n^{\mathrm{III}}(6) &= -w_n^{\mathrm{I}}(5) \\ w_n^{\mathrm{I}}(6) &= -w_n^{\mathrm{II}}(5) \\ w_n^{\mathrm{II}}(6) &= -w_n^{\mathrm{III}}(5) \end{aligned} \tag{2}$$

where superscripts refer to the subelements and the numbers in brackets to the nodes indicated in Figure 7.

These prescriptions could be imposed at other points and there could be more with polynomials of a higher degree than three. It has been proved[15] that it is not possible to enforce more than three conditions between subelements. In this family of finite elements the 3 d.o.f. at the centre of gravity, chosen to be dependent, are $w, \partial w/\partial x, \partial w/\partial y$.

Table I. D.O.F. distribution on an external side

	Function	A w(degree N)	B w_n(degree $N-1$)	A + B $w + w_n$
I	D.O.F. for C^1 continuity	$N+1$	N	$2N+1$
II	Corner d.o.f.	2×2	2×1	6
III = I − II	side d.o.f. excluding the corners	$N-3$	$N-2$	$2N-5$

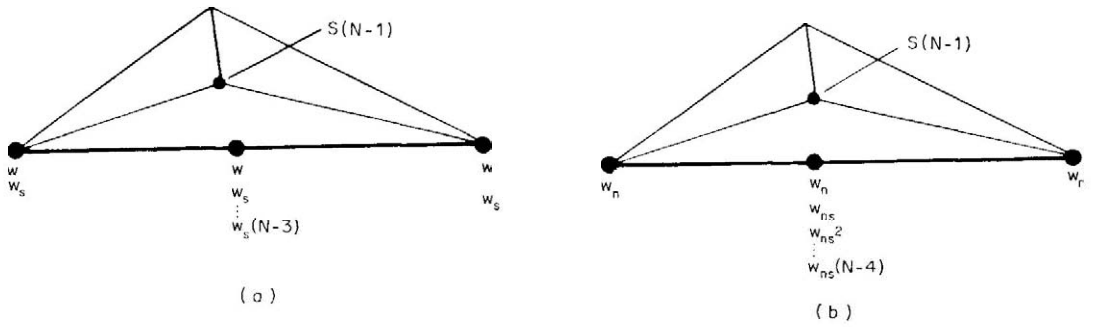

Figure 6. Continuity along an external side: (a) d.o.f. = $2 + 2 + N - 4 + 1 = N + 1$; number of constants in a polynomial of Nth order = $N + 1$; (b) d.o.f. = N; number of constants in a polynomial of $(N-1)$th order = N; d.o.f. at a node = $(N - 4 + 1) + (N - 3 + 1) = 2N - 5$; d.o.f. at the centre of gravity = $S(N+1) - 2 \times 3 - (2N-5) = S(N-1)$

Table II. D.O.F. distribution in an internal side

	Function	A w(degree N)	B w_n(degree $N-1$)	A + B $w + w_n$
I	D.O.F. for C^1 continuity	$N+1$	N	$2N+1$
II	D.O.F. at an external corner	2	1	3
III	D.O.F. at the centre of gravity, $S(N-1)$	$N-1$	$N-2$	$2N-3$
IV = II + III	D.O.F. on an internal side	$N+1$	$N-1$	$2N$

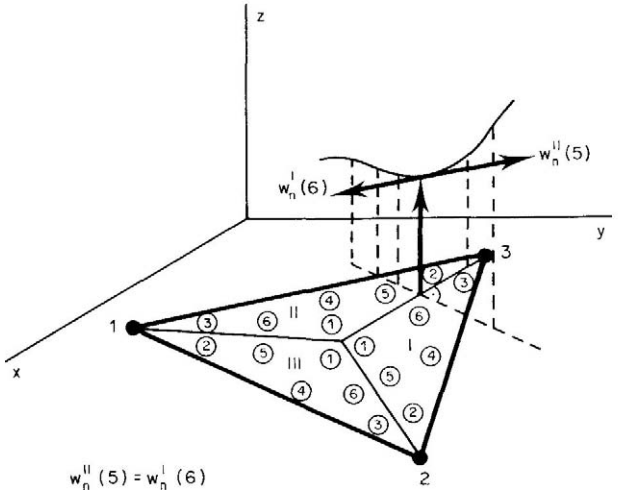

Figure 7. Internal continuity C^1

Analytical expression

As in a general F-E-M procedure, the general interpolation function is for each subelement.

$$w^{(i)} = \mathbf{L}\boldsymbol{\alpha}^{(i)} \tag{3}$$

where i means the number of the subelement, $\mathbf{L}$ is a vector of $S(N+1)$ components L_1^a, L_2^b, L_3^c (L_i are baricentric co-ordinates; see Figure 8 for $N=4$), $\boldsymbol{\alpha}$ is a vector of $S(N+1)$ constants α_{abc}.

If $\mathbf{d}$ are the d.o.f. (w and its derivatives) it can be obtained from (3) that

$$\mathbf{d}^{(i)} = \mathbf{C}^{(i)}\boldsymbol{\alpha}^{(i)} \tag{4}$$

and hence that

$$\boldsymbol{\alpha}^{(i)} = \bar{\mathbf{C}}^{(i)}\mathbf{d}^{(i)} \tag{5}$$

Then the interpolation function expression is

$$w^{(i)} = \mathbf{L}\bar{\mathbf{C}}^{(i)}\mathbf{d}^{(i)} = \boldsymbol{\phi}\mathbf{d}^{(i)} = \sum_{j=1}^{S(N+1)} \phi^j d_j^{(i)} \tag{6a}$$

From the vectors of d.o.f. of each subelement, $\mathbf{d}^{(i)}$, another vector $\mathbf{d}^*$ including all of them

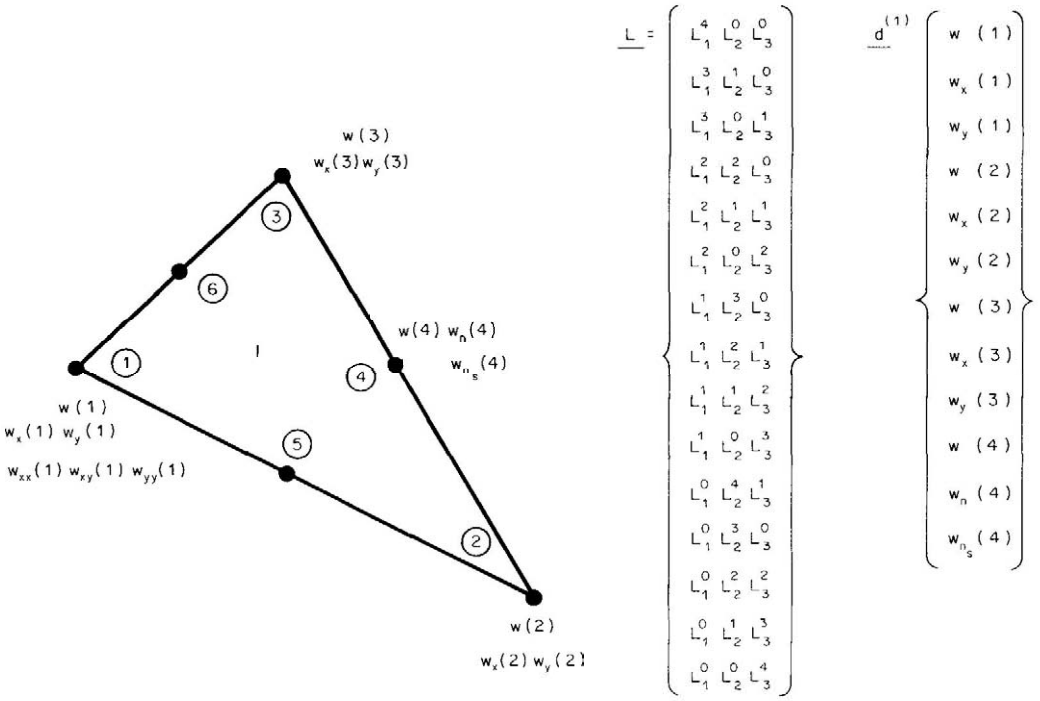

Figure 8. Baricentric interpolation coefficients for $N = 4$. Vectors $\mathbf{L}$ and $\mathbf{d}^{(1)}$

$(\mathbf{d}^{(1)}, \mathbf{d}^{(2)}, \mathbf{d}^{(3)})$ is formed, taking into account the fact that some d.o.f. are the same in different subelements. It is possible to divide $\mathbf{d}^*$ into two vectors $(\mathbf{d}_0^*, \mathbf{d}_1^*)^T$, so that $\mathbf{d}_0^*$ contains the linearly dependent d.o.f. and $\mathbf{d}_1^*$ the independent, after imposing C^1 continuity.

Equation (6a) now has another form:

$$w^{(i)} = \mathbf{L}\bar{\mathbf{C}}^{(i)}\mathbf{d}^{(i)} = \mathbf{L}(\bar{\mathbf{C}}_0^{(i)}, \bar{\mathbf{C}}^{(i)})(\mathbf{d}_0^*, \mathbf{d}_1^*)^T = \boldsymbol{\phi}^{(i)*}\mathbf{d}^* = \sum_{j=1}^{M} \phi^{(i)*j} d_j^* \tag{6b}$$

where

$$M = 3(3 + 2N - 5) + S(N - 1)$$

and the equation system (2) can be expressed as

$$\begin{aligned} \boldsymbol{\phi}_n^{(3)*}(6)\mathbf{d}^* &= -\boldsymbol{\phi}_n^{(1)*}(5)\mathbf{d}^* \\ \boldsymbol{\phi}_n^{(1)*}(6)\mathbf{d}^* &= -\boldsymbol{\phi}_n^{(2)*}(5)\mathbf{d}^* \\ \boldsymbol{\phi}_n^{(2)*}(6)\mathbf{d}^* &= -\boldsymbol{\phi}_n^{(3)*}(5)\mathbf{d}^* \end{aligned} \tag{7}$$

where

$$w_n = \boldsymbol{\phi}_n^{(i)*}\mathbf{d}^*$$

and hence

$$\begin{aligned} \mathbf{H}_0\mathbf{d}_0^* + \mathbf{H}_1\mathbf{d}_1^* &= \mathbf{0} \\ \mathbf{d}_0^* = -\mathbf{H}_0^{-1}\mathbf{H}_1\mathbf{d}_1^* &= \mathbf{H}\mathbf{d}_1^* \end{aligned} \tag{8}$$

so that (6b) becomes

$$w^{(i)} = \mathbf{L}(\bar{\mathbf{C}}_0^{(i)}\bar{\mathbf{C}}_1^{(i)})(\mathbf{H}\mathbf{d}_1^*, \mathbf{d}_1^*)^{\mathrm{T}} = \mathbf{L}(\bar{\mathbf{C}}_0^{(i)}\mathbf{H} + \bar{\mathbf{C}}_1^{(i)})\mathbf{d}_1^* = \mathbf{L}\mathbf{C}\mathbf{d}_1^* = \hat{\boldsymbol{\phi}}^{(i)}\mathbf{d}_1^* \tag{9}$$

The shape function $\hat{\boldsymbol{\phi}}^i$ corresponding to the displacement w at node 3 in a subelement for several degrees of polynomials is given in Figure 9.

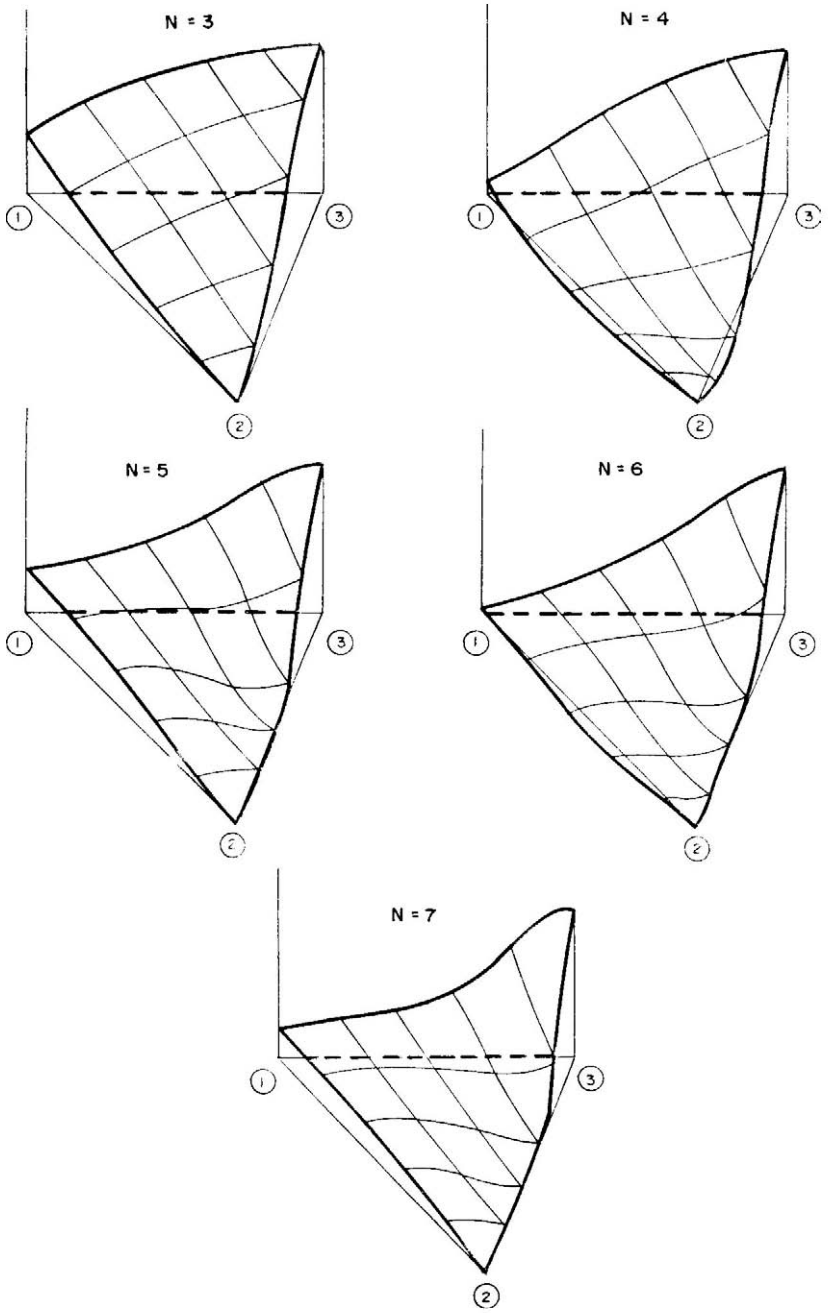

Figure 9. Deflection shape function $\phi^{(i)}$ at node 3 of a subelement

In Figure 10 the first three elements of the family are depicted.

Element stiffness matrix, static condensation and structural assembly

Using the plate governing equations and equations (9) the element stiffness matrix and equivalent forces are obtained. Owing to the fact that the internal node is not needed, the d.o.f. that are there can be eliminated by static condensation.

Afterwards the element stiffness matrices are added to generate the total stiffness matrix for the plate structure and in a similar way the complete equivalent force vector

$$\mathbf{P} = \mathbf{K}\mathbf{d} \tag{10}$$

where

$$\mathbf{K} = \sum_{i=1}^{n} \int\int_{A_i} (\mathbf{B}^i)^{\mathrm{T}} \mathbf{D} \mathbf{B}^i \, \mathrm{d}A$$

$$\mathbf{P} = \sum_{i=1}^{n} \left\{ \int\int_{A_i} \{ (\mathbf{B}^i)^{\mathrm{T}} \mathbf{D} \boldsymbol{\varepsilon}_0^i + (\boldsymbol{\psi}^i)^{\mathrm{T}} \mathbf{b} + (\boldsymbol{\psi}^i)^{\mathrm{T}} \mathbf{P} \} \, \mathrm{d}A_i + \int_{\bar{A} \wedge A_i} (\boldsymbol{\psi}^{i\mathrm{T}}) \mathbf{P} \mathbf{s} \, \mathrm{d}s \right\} \tag{11}$$

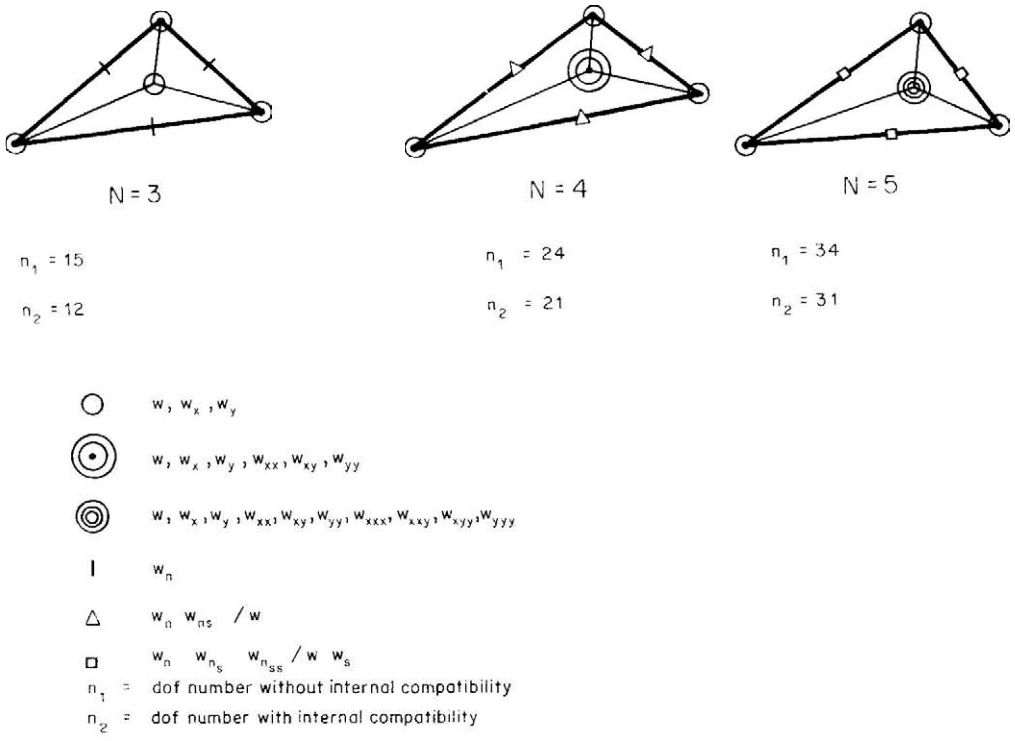

Figure 10. The first three elements of the family

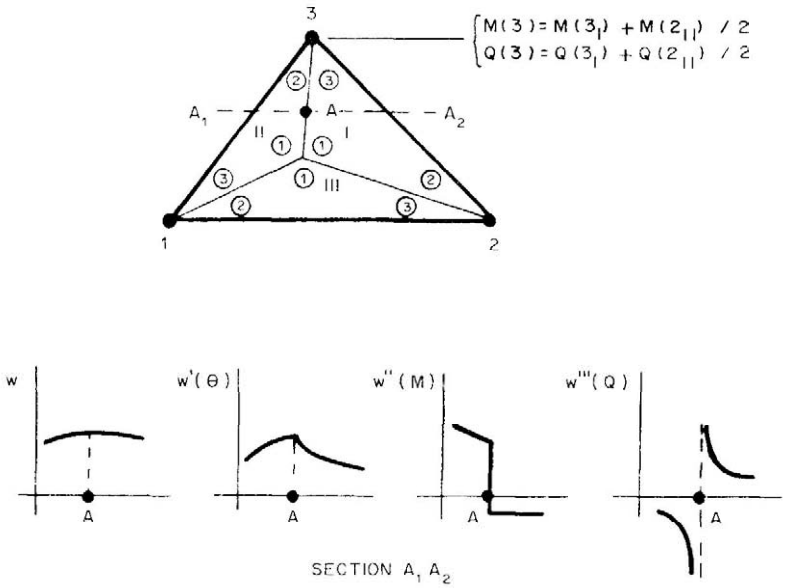

Figure 11. Evaluation of the results

Results

As there are three subtriangles in each subelement, there are three groups of shape functions as well. There are no problems in deflection (w) and its first-order derivatives on the frontier between subelements, so that C^1 continuity exists. In the second- and third-order derivatives, that represent the bending moment and the shear force, there is no continuity. Thus the average of the subelement results has been made (Figure 11).

The element stiffness matrix has been used as well in order to obtain the results. The accuracy is improved, especially in the shear force.

NUMERICAL RESULTS

Numerical results

The elements of this family have been applied to numerous cases in order to know their performance in relation to several variables: influence of the load type, boundary conditions, skewness of the elements, relation between the lengths of the sides and mesh patterns.

Loading and boundary conditions. As an example a typical case is tested: a square plate of side a with Poisson's ratio equal to 0·3. Two cases are presented: a built-in plate along the boundary with a uniform load of intensity q (Table III), and a plate, supported simply by its corners under a point load P at the centre (Table IV).

Skewness. In order to check the performance of these elements with irregular geometry for the analysis of skew plates under uniform loading with two of the opposite edges simply supported and the other two free, three different kinds of examples have been examined. In order to avoid a large computational effort the experimentation was carried out with only four elements and poly-

Table III. Square plate: boundary built-in

Mesh type:
a: side length
q: uniform load intensity
ν: 0·3 (Poisson's ratio)
w: centre deflection
M: centre moment
M_1, M_2: centre side moments

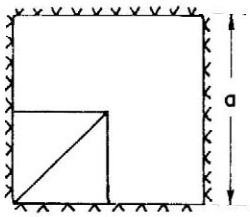

Q: middle side shear
R: middle side Kirchhoff reactions
DOF1: total number of d.o.f.
DOF2: number of active d.o.f.
NDEG: polynomial degree

NDEG	DOF1	DOF2	w	M	M_1	M_2	Q	R
3	17	2	0·0005422	0·01480	−0·003904	−0·01301	0·05205	0·04750
4	27	6	0·0012921	0·03343	−0·01123	−0·03744	0·2221	0·2302
5	37	10	0·001265	0·02466	−0·01511	−0·05038	0·4319	0·4540
6	47	14	0·001263	0·02056	−0·01547	−0·05156	0·4515	0·4714
7	57	18	0·001266	0·02410	−0·01546	−0·05152	0·4545	0·4672
Exact[16]			0·00126	0·0231	−0·01540	−0·0513	0·4405[17]	0·4403[17]
Coefficient			qa^4/D	qa^2	qa^2	qa^2	qa	qa

Table IV. Square plate: simply supported corners Mesh type:

a: side length
P: centre point load intensity
ν: 0·3 (Poisson's ratio)
w: centre deflection
w_1: centre side deflection

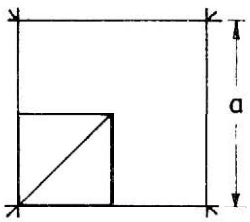

M: centre moment
R_c: corner reaction
DOF1: total number of d.o.f.
DOF2: number of active d.o.f.
NDEG: polynomial degree

NDEG	DOF1	DOF2	w	w_1	M	R_c
3	17	11	0·03765	0·02282	0·02569	0·13612
4	27	19	0·03891	0·02286	0·2067	0·2658
5	37	28[7]	0·03907	0·02291	0·2009	0·2100
6	47	35	0·03911	0·02291	0·2038	0·2540
7	57	43	0·03912	0·02291	0·2017	0·2260
Exact SAP4	LCCT9		0·0390	0·02284	0·16217[17]	0·2430[17]
Coefficient			Pa^2/D	Pa^2/D	P/a	P/a

Table V. Skew plate

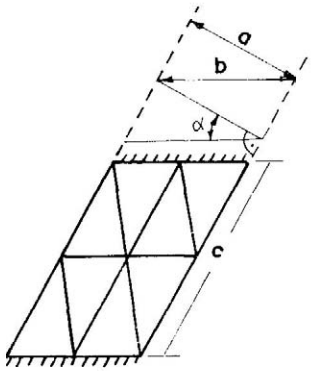

Mesh type:
b: simply supported side
c: free side
b, *c*: sides lengths
q: uniform load intensity

v: 0·3 (Poisson's ratio)
w: centre deflection
M: centre moment
DOF1: total number of d.o.f.
DOF2: number of active d.o.f.
NDEG: polynomial degree.

			$\alpha = 30°$ $b = 1{\cdot}5a$ $c = 1{\cdot}9245a$		$\alpha = 45°$ $b = 1{\cdot}41a$ $c = 2a$		$\alpha = 60°$ $b = 2a$ $c = 2a$	
NDEG	DOF1	DOF2	*w*	*M*	*w*	*M*	*w*	*M*
3	43	31	0·1045	0·46850	0·06642	0·29507	0·01487	0·12848
4	75	59	0·1052	0·46789	0·06935	0·31064	0·01742	0·16652
Exact[18]			0·1183	0·368	0·07080	0·291	0·01860	0·1660
Coefficient			qa^4/D	qa^2	qa^4/D	qa^2	qa^4/D	qa

nomials of degree no higher than the fourth. The accuracy obtained in the results can only indicate the tendency. The results are shown in Table V.

Different side relationships. The influence of the ratio between the lengths of the sides is shown in Table VI for a simply supported rectangular plate with uniform load.

Mesh dependence. The importance of the type of mesh pattern is depicted in Figure 12 for a square built-in plate under uniform loading. The best results are obtained from the C mesh type, especially 1 C and 2CE. Similar results could be shown for a simply supported square plate under point loading. In any case the monotonous convergence is ensured because the elements are C^1.

Comparative study with other elements

In order to assess not only the speed of convergence of this family of the elements but its possible computational efficiency as well, a comparative study with other elements is carried out. The comparative variable is the number of d.o.f.; however it does not represent the total computational effort, because in high-order polynomials the generation of the stiffness matrix demands considerable computer time.

The results are depicted in Figures 13 and 14. They are related only to bending moment and central deflection. The results for the shear force are not normally published since their error rate is usually fairly high. However the results obtained with this family are quite accurate even for the shear force.

Table VI. Rectangular plate: boundary simply supported

Mesh type:
a, b: side lengths
q: uniform load intensity
ν: 0·3 (Poisson's ratio)
w: centre deflection
$M_1 M_2$: centre moments

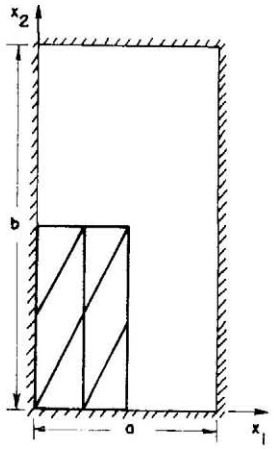

$Q_1 Q_2$: centre side shear
$R_1 R_2$: centre side Kirchhoff reactions
DOF1: total number of d.o.f.
DOF2: number of active d.o.f.
NDEG: polynomial degree

b/a	NDEG	DOF1	DOF2	w	M_1	M_2	Q_1	Q_2	R_1	R_2
1·5	3	43	24	0·007594	0·07633	0·04223	0·2293	0·1485	0·2808	0·2419
	4	75	48	0·007724	0·08101	0·04989	0·4485	0·3477	0·5196	0·4764
	Exact[19]			0·00772	0·0812	0·0498	0·424	0·363	0·486	0·480
2·0	3	43	24	0·009996	0·09480	0·03940	0·2841	0·1295	0·3200	0·2268
	4	75	48	0·01013	0·1016	0·04651	0·4990	0·3249	0·5426	0·4666
	Exact[19]			0·01013	0·1017	0·0464	0·465	0·370	0·503	0·496
3·0	3	43	24	0·01221	0·1163	0·03757	0·3519	0·1006	0·3681	0·1852
	4	75	48	0·01223	0·1189	0·04071	0·5346	0·2618	0·5469	0·4083
	Exact[19]			0·01223	0·1189	0·0406	0·493	0·372	0·505	0·498
	Coefficients			qa^4/D	qa^2	qa^2	qa	qa	qa	qa

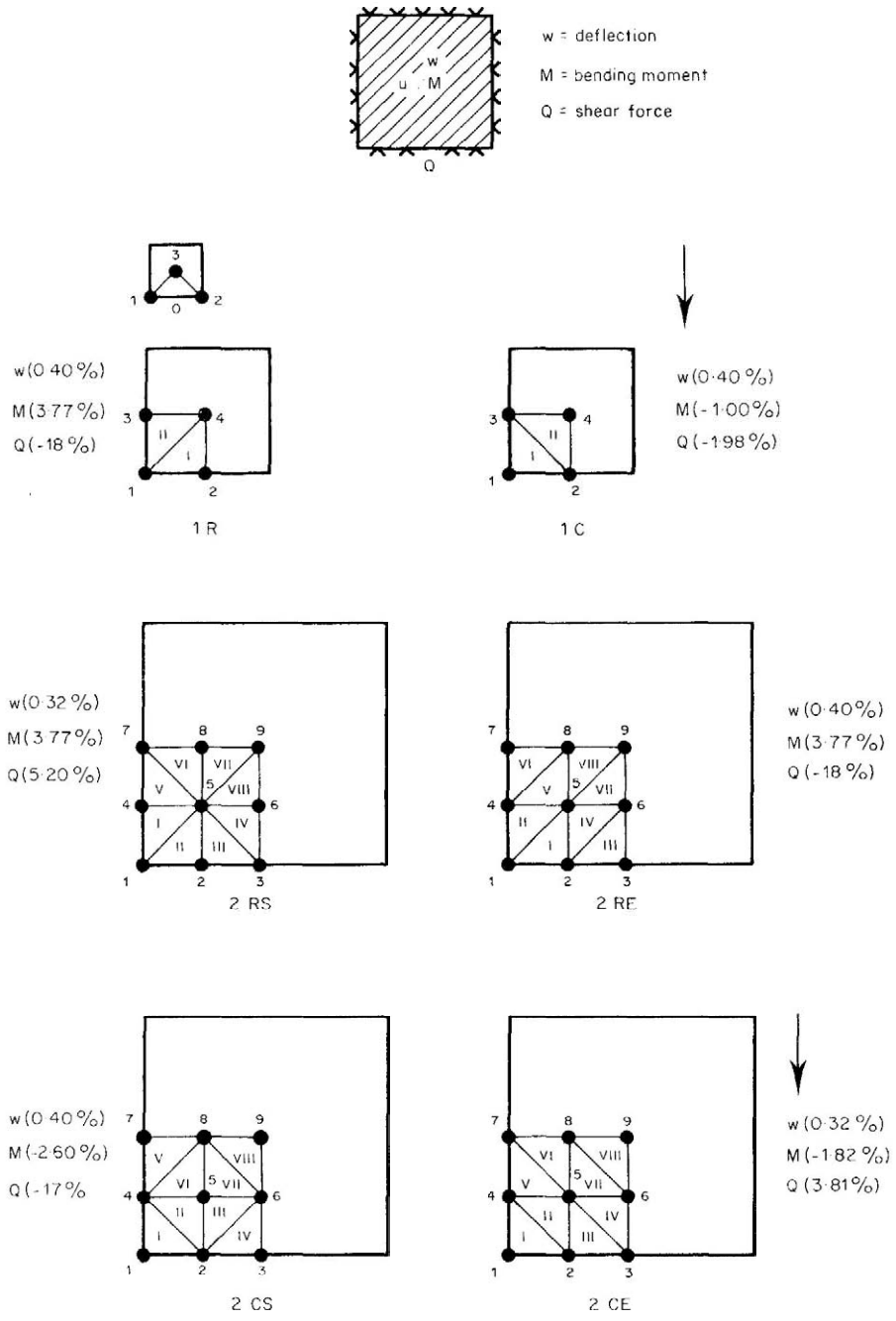

Figure 12. Mesh types

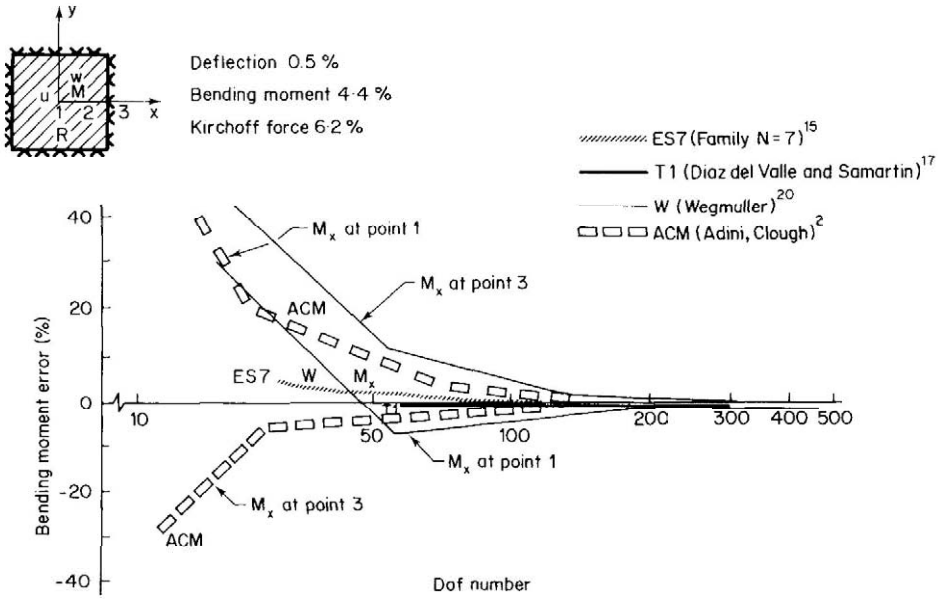

Figure 13. Bending moment error (per cent) versus number of d.o.f. for a built-in square plate under uniform load

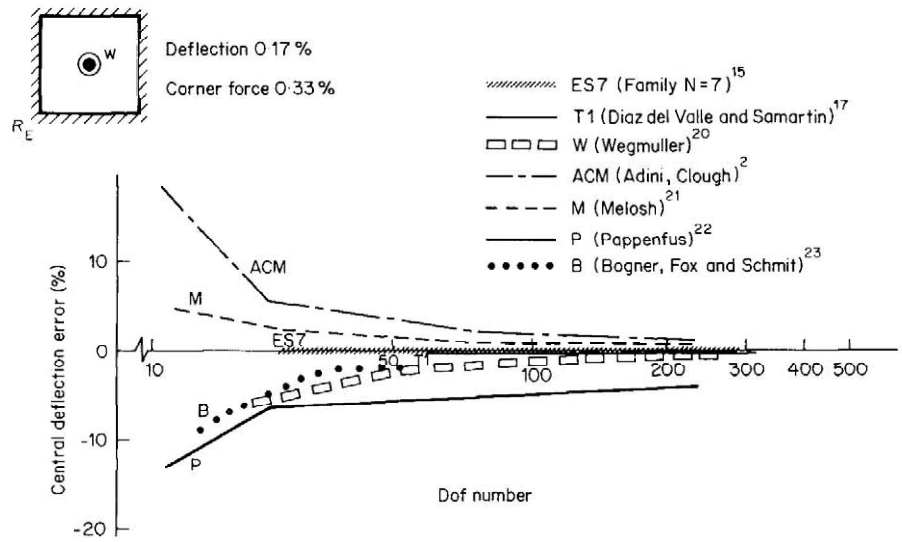

Figure 14. Central deflection error (per cent) versus number of d.o.f. for the simply supported square plate under point-loading at the centre

APPLICATIONS AND CONCLUSIONS

With this family it is possible to reach convergence in two different ways, first by refinement of the mesh (h-convergence) as in any other case, and secondly by an increase in the order of the interpolation polynomial in the element (h^k-convergence). It has been shown above that the latter seems to be more efficient. This holds particularly if the elements are equally repeated throughout

the domain, because the effort to obtain its stiffness matrices is drastically reduced if they are computed only once.

In comparison with hyperelements, this family has the advantage that the sharp jumps in elastic or thickness characteristics can be easily considered. However the accuracy in the results, which imply higher derivatives, is better in hyperelements because they are the d.o.f. Even though it is possible to have the dual results (high order derivatives) of the d.o.f. by using the stiffness matrix.

The results have been obtained with polynomials between the third and seventh degrees and using numerical integration. It has been observed that high order derivatives present a great sensitivity and numerical noise may appear.

It is also very easy to use this family in shells as the high order derivatives have direct compatibility.[11]

POSSIBLE EXTENSIONS

Some practical tables for special boundary conditions, changing of thickness, and elastic constants are to be made with the use of these elements.

The intersubelement continuity achieved is C^1. The possible maximum is still open to study.[24] The analysis of the influence of the choice of d.o.f. to be eliminated at the centre node in order to obtain the internal continuity is to be carried out.

The noise produced in high order derivatives is to be assessed, especially for the matrix conditioning.

The results for the variables that are not d.o.f. can be obtained (a) by using shape functions at the point, (b) by using the shape functions and their values at the integration points, (c) by means of the stiffness matrix for the dual variables of the d.o.f. A comparison between these three methods would be of great interest.[9] Some results of the third method have shown a very good accuracy.

The extension to curved compact supports would be very useful for the case of irregular boundaries.

The extensive numerical experimentation has been carried out only with polynomials of degree less than seven because the integration tables for triangles are not available for higher degrees. The extension of these tables to higher degree polynomials would be very interesting.

The use of several kinds of elements within the family can relieve some computational effort. Low degree elements can be used near the boundary, normally in large numbers in order to model the geometry, and only a few high degree elements are usually required in the central area of the plate. Obviously the hierarchic family should include transitional elements. These can be obtained either directly or from a normal element by reduction of the order along some sides of the element.

In order to allow the simultaneous use of elements of different orders, the introduction of a general nomenclature in the hierarchic families may be useful.

ACKNOWLEDGEMENTS

The authors wish to acknowledge the comments of the reviewers that have helped to improve the clarity of this paper.

APPENDIX

Triangles formulation

The values shown in Figure 15, considering cyclic permutation ($i = 1, 2, 3, j = 2, 3, 1, k = 3, 1, 2,$), are as follows

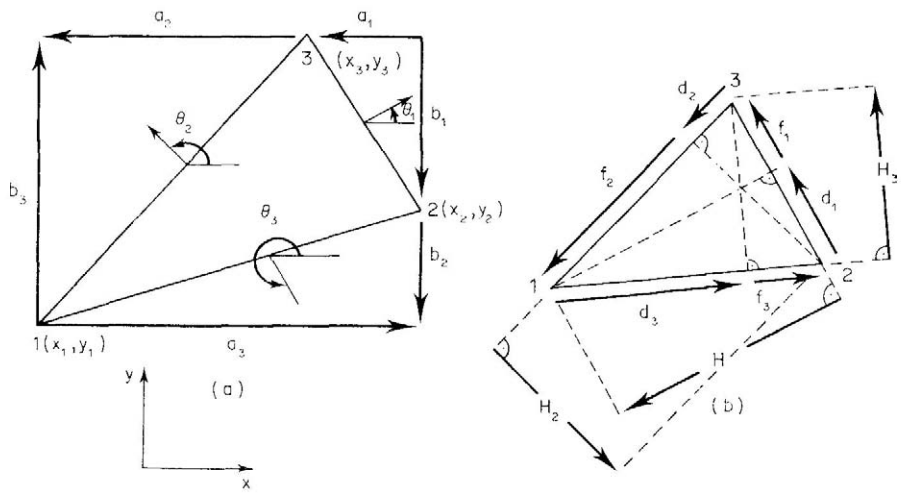

Figure 15. Triangle parameters

$$a_i = x_k - x_j$$
$$b_i = y_j - y_k$$

with

$$\sum_{i=1}^{3} a_i = \sum_{i=1}^{3} b_i = 0$$

$$a_i = -(a_j + a_k)$$

$$b_i = -(b_j + b_k)$$

$$d_i = a_k \sin\theta_i + b_k \cos\theta_i = \frac{a_i a_k + b_i b_k}{e_i}$$

$$e_i = a_i \sin\theta_i + b_i \cos\theta_i = \sqrt{(a_i^2 + b_i^2)}$$

$$f_i = a_j \sin\theta_i + b_j \cos\theta_i = \frac{a_i a_j + b_i b_j}{e_i}$$

$$H_i = a_k \cos\theta_i - b_k \sin\theta_i = \frac{a_i b_j - b_i a_j}{e_i}$$

$$-H_i = a_j \cos\theta_i - b_j \sin\theta_i = \frac{a_i b_k - b_i a_k}{e_i}$$

where

$$d_i + f_i + e_i = 0$$

The triangle area and intrinsic co-cordinates are (for $i = 1, 2, 3$)

$$2A = a_i b_k - b_i a_k = -(a_i b_j - b_i a_j)$$

$$\lambda_i = \frac{d_i}{-e_i}$$

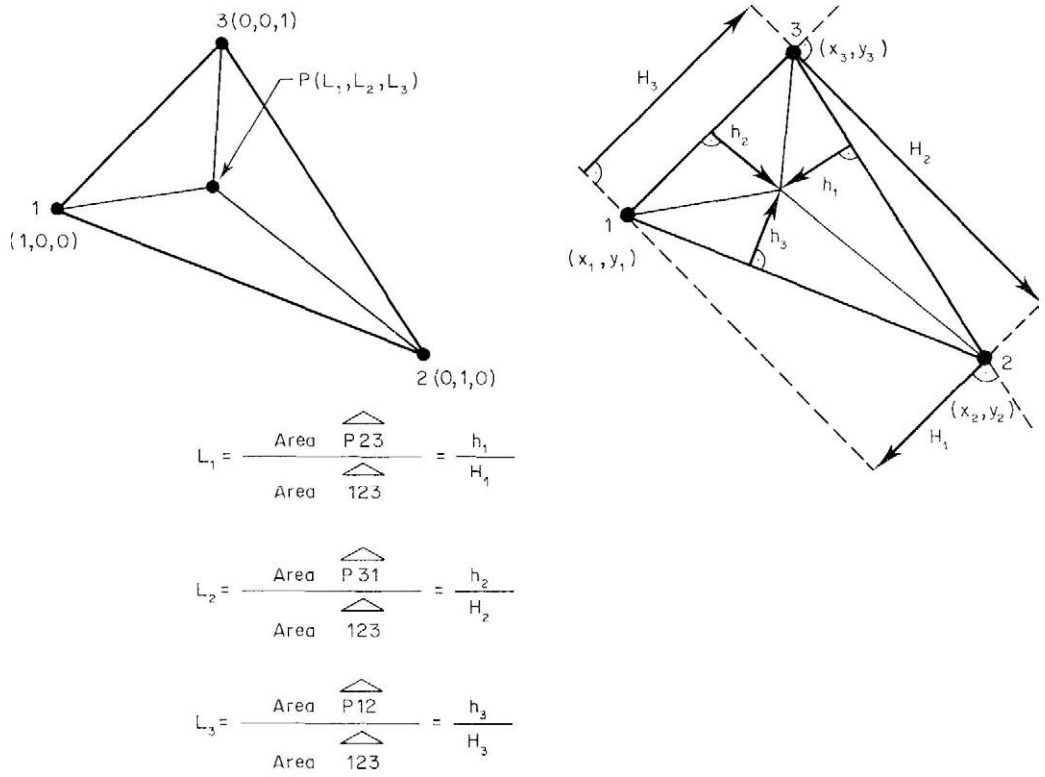

Figure 16. Triangular co-ordinates

$$\mu_i = 1 - \hat{\lambda}_i = \frac{d_i}{-e_i}$$

The relationship between the triangular and Cartesian co-ordinate systems (Figure 16) is as follows:

$$\begin{bmatrix} L_1 \\ L_2 \\ L_3 \end{bmatrix} = \frac{1}{2A} \begin{bmatrix} 2A_{23} & b_1 & a_1 \\ 2A_{31} & b_2 & a_2 \\ 2A_{12} & b_3 & a_3 \end{bmatrix} \begin{bmatrix} 1 \\ x \\ y \end{bmatrix}$$

where

$$2A_{ij} = x_i y_j - x_j y_i$$

and the inverse transformation is

$$\begin{bmatrix} 1 \\ x \\ y \end{bmatrix} = \begin{bmatrix} 1 & 1 & 1 \\ x_1 & x_2 & x_3 \\ y_1 & y_2 & y_3 \end{bmatrix} \begin{bmatrix} L_1 \\ L_2 \\ L_3 \end{bmatrix}$$

The relationship between general and side Cartesian co-ordinates (Figure 17) is

$$\begin{bmatrix} n_i \\ s_i \end{bmatrix} = \frac{1}{e_i} \begin{bmatrix} +b_i & a_i \\ -a_i & b_i \end{bmatrix} \begin{bmatrix} x - x_j \\ y - y_j \end{bmatrix}$$

$$\begin{bmatrix} x \\ y \end{bmatrix} = \frac{1}{e_i} \begin{bmatrix} b_i & -a_i \\ a_i & b_i \end{bmatrix} \begin{bmatrix} n_i & x_j \\ s_i & y_j \end{bmatrix}$$

Following Figure 18, side Cartesian co-ordinates and triangular co-ordinates are related by

$$\begin{bmatrix} n_i \\ s_i \\ 1 \end{bmatrix} = \begin{bmatrix} -H_i & 0 & 0 \\ d_i & -e_i & 0 \\ 1 & 1 & 1 \end{bmatrix} \begin{bmatrix} L_i \\ L_k \\ L_j \end{bmatrix}$$

$$\begin{bmatrix} L_i \\ L_k \\ L_j \end{bmatrix} = \frac{1}{2A} \begin{bmatrix} e_i & 0 & 0 \\ d_i & H_i & 0 \\ f_i & -H_i & 2A \end{bmatrix} \begin{bmatrix} n_i \\ s_i \\ 1 \end{bmatrix}$$

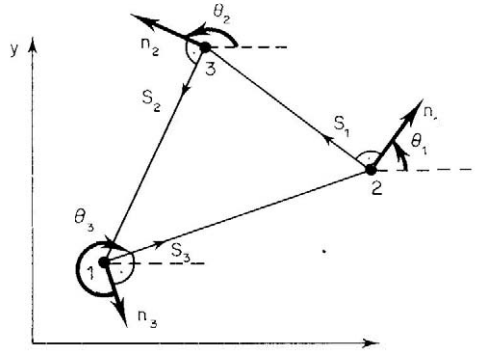

Figure 17. Side Cartesian co-ordinates

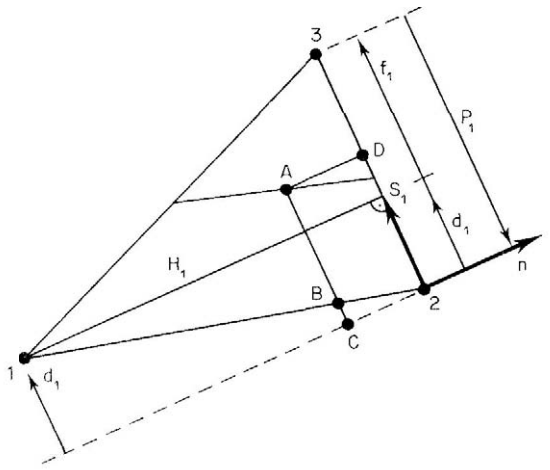

$n_1 = |\overline{AD}|$

$S_1 = |\overline{AB}| + |\overline{BC}|$

$|\overline{AD}| = H_1 L_1$

$|\overline{AB}| = -e_1 L_3$

$|\overline{BC}| = d_1 L_1$

Figure 18

The interco-ordinate derivatives are

$$\frac{\partial L_i}{\partial x} = \frac{b_i}{2A}, \quad \frac{\partial L_i}{\partial y} = \frac{a_i}{2A}$$

$$\frac{\partial L_i}{\partial n_i} = \frac{e_i}{2A}, \quad \frac{\partial L_i}{\partial s_i} = 0$$

$$\frac{\partial L_j}{\partial n_i} = \frac{f_i}{2A}, \quad \frac{\partial L_j}{\partial s_j} = \frac{-H_i}{2A}$$

$$\frac{\partial L_k}{\partial n_i} = \frac{d_i}{2A}, \quad \frac{\partial L_k}{\partial s_i} = \frac{H_i}{2\mathrm{A}}$$

The parameters and triangular co-ordinates of subelements and the complete element are related as follows (Figure 19, in which centre number 3 is the baricentre):

$$a_1^{(i)} = -a_2^{(j)} = x_k = -x_i + a_j$$

$$a_2^{(i)} = -a_1^{(k)} = +x_j = x_i + a_k$$

$$a_3^{(i)} = a_i$$

$$b_1^{(i)} = -b_2^{(j)} = y_k = y_i + b_j$$

$$b_2^{(i)} = -b_1^{(k)} = -y_j = -y_i + b_k$$

$$b_3^{(i)} = b^i$$

As the node 3 of each subelement is the baricentre:

$$x_1 + x_2 + x_3 = 0$$

$$y_1 + y_2 + y_3 = 0$$

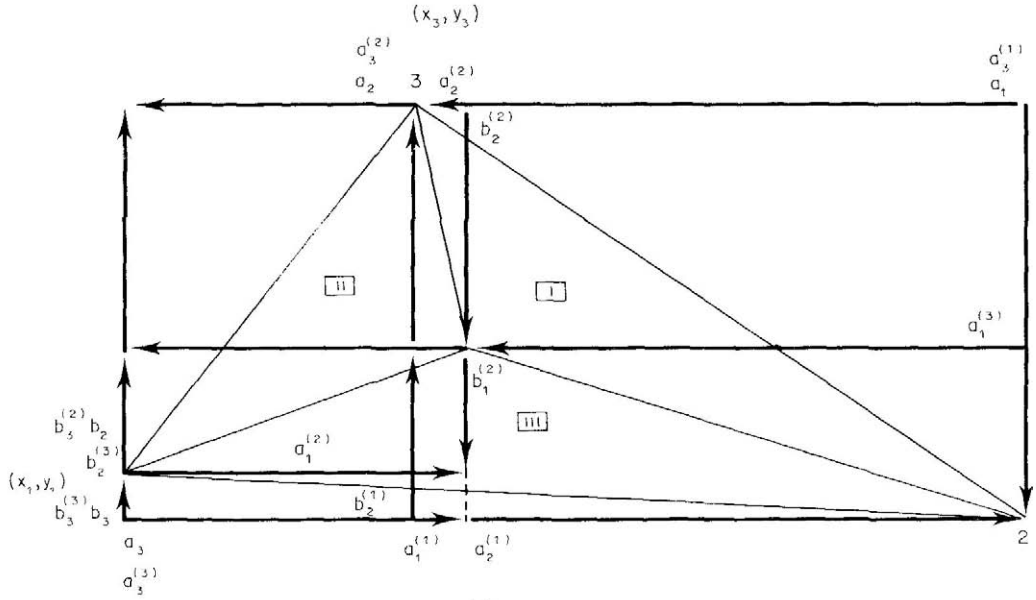

Figure 19

Thus we have:

$$a_1^{(i)} = \frac{a_j - a_i}{3}, \qquad b_1^{(i)} = \frac{b_j - b_j}{3}$$

$$a_2^{(i)} = \frac{a_k - a_i}{3}, \qquad b_2^{(i)} = \frac{b_k - b_i}{3}$$

$$a_3^{(i)} = a_i, \qquad b_3^{(i)} b_i$$

and for the triangular co-ordinates (Figure 20)

$$L_i^{(i)} = 3L_i, \qquad L_i = \frac{L_i^{(i)}}{3}$$

$$L_j^{(i)} = \frac{1}{2} - \frac{3}{2}L_i + \frac{L_j}{2} - \frac{L_k}{2}, \qquad L_j = \frac{1}{2} - \frac{L_i^{(i)}}{6} + \tfrac{1}{2}L_j^{(i)} - \tfrac{1}{2}L_k^{(i)}$$

$$L_k^{(i)} = \frac{1}{2} - \frac{3}{2}L_i - \frac{L_j}{2} + \frac{L_k}{2}, \qquad L_k = \frac{1}{2} - \frac{L_i^{(i)}}{6} + \tfrac{1}{2}L_j^{(i)} - \tfrac{1}{2}L_k^{(i)}$$

Expression of a polynomial and its derivatives

polynomial. If $S(N) = N(N+1)/2$

$$p(L_1, L_2, L_3) = \sum_{\substack{i,j,k=0 \\ i+j+k=N}} \lambda_{ijk} L_1^i L_2^j L_3^k = \sum_{n=1}^{S(N+1)} \alpha N_n LN_n$$

where

$$i = i(N,n), \quad j = j(N,n), \quad k = k(N,n)$$

Natural derivatives.

$$p_m = \frac{\partial^{\alpha+\beta+\gamma} p}{\partial L_1^\alpha \partial L_2^\beta \partial L_3^\gamma} = \sum_{n=1}^{S(N+1)} \alpha N_n \frac{i!}{(i-\alpha)!} \frac{j!}{(j-\beta)!} \frac{k!}{(k-\gamma)!}$$

it is a product

$$L_1^{(i-\alpha)} L_2^{(j-\beta)} L_3^{(k-\gamma)} = \sum_{n=1}^{S(N+1)} \alpha N_n \frac{i!}{(i-\alpha)!} \frac{j!}{(j-\beta)!} \frac{k!}{(k-\gamma)!} LN_{n,\alpha\beta\gamma}$$

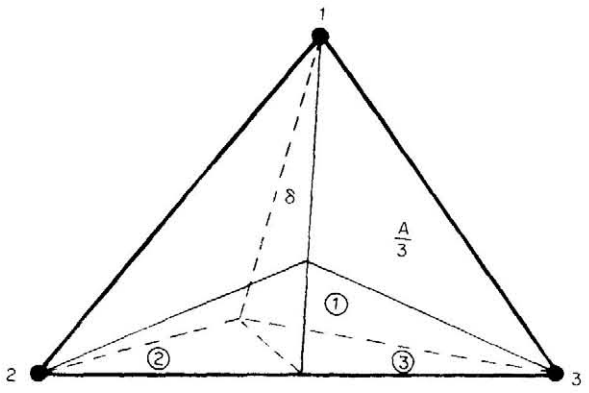

Figure 20

where

$$LN_{n,\alpha\beta\gamma} = 0 \quad \text{if} \quad i < \alpha \quad \text{or} \quad j < \beta \quad \text{or} \quad k < \gamma$$
$$\alpha = \alpha(m), \quad \beta = \beta(m), \quad \gamma = \gamma(m)$$

General Cartesian derivatives.

$$\bar{p}_m = \frac{\partial^{j+k} p}{\partial \bar{x}^j \partial \bar{y}^k} = \left\{ \frac{1}{2A} (b_1 p_{,L_1} + b_2 p_{,L_2} + b_3 p_{,L_3}) \right\}^{(j} \left\{ \frac{1}{2A} (a_1 p_{,L_1} + a_2 p_{,L_2} + b_3 p_{,L_3}) \right\}^{(k}$$

with

$$j = j(m), \qquad k = k(m)$$

$$\bar{p}_m = \left(\frac{1}{2A} \right)^{j+k} \sum_{\nu=1}^{S(j+1)} \sum_{\mu=1}^{S(k+1)} A_{j\nu} B_{k\mu} \frac{\partial^{j+k} p}{\partial L_1^{j_1+k_1} \partial L_2^{j_2+k_2} \partial L_3^{j_3+k_3}}$$

with

$$A_{j\nu} = \frac{j!}{j_1! j_2! j_3!} b_1^{j_1} b_2^{j_2} b_3^{j_3}$$

$$B_{k\mu} = \frac{k!}{k_1! k_2! k_3!} a_1^{k_1} a_2^{k_2} a_3^{k_3}$$

and

$$j_1 = j_1(j, \nu), \qquad j_2 = j_2(j, \nu), \qquad j_3 = j_3(j, \nu)$$
$$k_1 = k_1(k, \mu), \qquad k_2 = k_2(k, \mu), \qquad k_3 = k_3(k, \mu)$$

Local Cartesian derivatives.

$$\bar{p}^i_m = \frac{\partial^{j+k} p}{\partial s_i^j \partial n_i^k} = \left\{ \frac{1}{2A} (a_{i1} p_{,L_1} + a_{i2} p_{,L_2} + a_{i3} p_{,L_3}) \right\}^{(j} \times \left\{ \frac{1}{2A} (b_{i1} p_{,L_1} + b_{i2} p_{,L_2} + b_{i_3} p_{L_3}) \right\}$$

with

$$j = j(m), \qquad k = k(m)$$
$$a_{ii} = 0, \qquad a_{ij} = -H_i, \qquad a_{ik} = H_i \quad \text{and} \quad (0^0 = 1)$$
$$b_{ii} = e_i, \qquad b_{ij} = f_i, \qquad b_{ik} = d_i$$

and i is the number of side.

$$\bar{p}^i_m = \left(\frac{1}{2A} \right)^{j+k} \sum_{\nu=1}^{S(j+1)} \sum_{\mu=1}^{S(k+1)} \bar{A}^i_{j\nu} \bar{B}^i_{k^\mu} \frac{\partial^{j+k} p}{\partial L_1^{j_1+k_1} \partial L_2^{j_2+k_2} \partial L_3^{j_3+k_3}}$$

with

$$\bar{A}^i_{j\nu} = \frac{j!}{j_1! j_2! j_3!} (a_{i1})^{j_1} (a_{i2})^{j_2} (a_{i3})^{j_3}$$

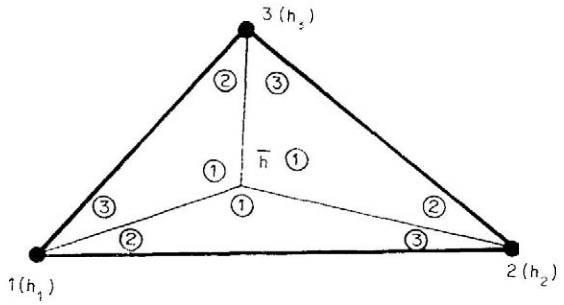

Figure 21. Thicknesses

$$\bar{B}^i_{k\mu} = \frac{k!}{k_1!k_2!k_3!}(b_{i1})^{k_1}(b_{i2})^{k_2}(b_{i3})^{k_3}$$

and

$$j_1 = j_1(j,\nu), \quad j_2 = j_2(j,\nu), \quad j_3 = j_3(j,\nu)$$
$$k_1 = k_1(k,\mu), \quad k_2 = k_2(k,\mu), \quad k_3 = k_3(k,\mu)$$

Thickness

The variation of thickness can be modelled as follows (Figure 21):

$$\bar{h} = h(\tfrac{1}{3},\tfrac{1}{3},\tfrac{1}{3}) = \frac{h_1 + h_2 + h_3}{3}$$

In the subelement number i:

$$h^{(i)}(L_1^{(i)}, L_2^{(i)}, L_3^{(i)}) = \bar{h}L_1^{(i)} + h_j L_j^{(i)} + h_k L_k^{(i)}$$

REFERENCES

1. O. C. Zienkiewicz, *The Finite Element Method in Engineering Science*, McGraw-Hill, London, 1979.
2. A. Adini and R. W. Clough, 'Analysis of plate bending by the finite element method', A Report to the National Science Foundation, U.S.A., G. 7337, 1961.
3. G. P. Bazeley, Y. K. Cheun, B. M. Irons and O. C. Zienkiewicz, 'Triangular elements in bending conforming and non-conforming solution', *Proc. Conf. Matrix Methods in Struct. Mech.*, Air Force Inst. of Tech., Wright-Patterson A. F. Base, Ohio, October 1965.
4. B. M. Irons, 'The patch test for engineers', *Conf. Atlas Computing Centre*, Harwell U.I., March 1974.
5. B. M. Irons and M. Loikkanen, 'An engineers' defence of the patch test', *Int. j. numer. methods eng.*, **19**, 1391–1401 (1983).
6. B. M. Irons and J. K. Draper, 'Inadequacy of nodal connections in a stiffness solution for plate bending', *J.A.I.A.A.*, **3**, 5 (1965).
7. J. L. Batoz, K. J. Bathe and L. W. Ho, 'A study of three-node triangular plate bending elements', *Int. j. numer. methods eng.*, **15**, 1771–1812 (1980).
8. A. K. Noor and W. D. Plikey, 'State of the art surveys of finite element methods', *AMD Special Publication*, 1981.
9. A. Peano, 'Conforming approximations for Kirchhoff plates and shells', *Int. j. numer. methods eng.*, **14**, 1273–1291 (1979).
10. A. Samartín, 'Aplicación del método de los elementos finitos al análisis estructural de puentes', *Discurso de inauguración de Curso Académico 1979–80*, Universidad de Santander, 1979.
11. J. F. Moya, P. Fuster and S. Monleón, 'Una teoría variacional para el análisis de láminas hiperelásticas basada en una jerarquización a orden N del modelo cinemático transversal. Aplicación de primer orden al estudio del comportamiento no lineal y de la establidad', *E.T.S. de Ing. de Caminos*, Universidad Politécnica de Valencia, Junio 1984.
12. R. W. Clough and J. L. Tocher, 'Finite element stiffness matrices for analysis of plate bending', *Proc. Conf. Matrix*

Methods in Struct. Mech., Air Force Inst. of Tech., Wright-Patterson A.F. Base, Ohio. 1965.
13. R. Clough and C. Felippa, 'A refined quadrilateral element for analysis of plate bending', *Proc. II. Conf. Matrix Methods in Struct. Mech.*, Air Force Inst. of Tech., Wright-Patterson A.F. Base, Ohio, 1968.
14. A. Samartin, 'Un estudio sobre la exacitud del método de los elementos finitos. Aplicación a la barra de sección variable bajo esfuerzos axiles'. Universidad de Santander. Noviembre de 1980.
15. J. Torres, 'Una familia de elementos simples conformes clase C^1', *Ph.D. Dissertation*, Dept. de Análisis de la Estructuras, E.T.S. de Ing. de Caminos de Santander, 1984.
16. T. H. Evans, *Journal Appl. Mechanics*, **6**, A-7 (1939).
17. J. Díaz del Valle and A. Samartin, 'Una contribución al estudio de hiperelementos finitos en placas', *Ph.D. Dissertation*, Departamento de Análisis de las Estructuras de la E.T.S. de Ing. de Caminos, Santander, 1980.
18. U. P. Jensen, *Bulletin 332*, Illinois University, 1941.
19. S. Timoshenko and S. Woinowsky-Krieger, *Theory of Plates and Shells*, McGraw-Hill, 2nd edn, 1959.
20. A. Vegmulier, 'Finite element analysis of elastic plastic plates and eccentrically stiffened plates', *Ph.D. Dissertation*, Civil Eng. Dept. Lehigh University, 1971.
21. R. J. Melosh, 'A stiffness matrix for the analysis of thin plates in bending', *Journal of Aeronautical Sciences*, **28**, 34 (1961).
22. S. W. Papperfusn, 'Lateral plate deflection by stiffness matrix methods with application to a marqee'. *M.S. Thesis*, Dept. of Civil Eng., University of Washington, Seatle 1969.
23. F. K. Bogner, R. L. Fox and L. A. Schmit, 'The generation of interelement compatible stiffness and mass matrices by the use of interpolation formulas', *Proc. First. Conf. on Matrix Methods in Struct. Mech.*, Wright-Patterson A.F. Base, Ohio, November 1965.
24. M. Gasca and J. I. Maeztu, 'On Lagrange and Hermite interpolation in R^k', *Numer. Math.*, **39**, 1–14 (1982).
25. J. García de Jalón, 'Contribución a la resolución numérica del problema termoelástico en sólidos con simertía de revolución', *Ph.D. Dissertation*, E.T.S. Ing. Industriales, San Sebastián, 1977.
26. B. M. Irons, 'A conforming quartic triangular element for plate bending', *Int. j. numer. methods eng.*, **1**, 29–45 (1969).